High quality beam produced by tightly focused laser driven wakefield accelerators

Jia Wang, Ming Zeng,* Dazhang Li,† Xiaoning Wang, and Jie Gao

Institute of High Energy Physics, Chinese Academy of Sciences, Beijing 100049, China and University of Chinese Academy of Sciences, Beijing 100049, China

(Received 23 April 2023; accepted 5 September 2023; published 26 September 2023)

We propose to use tightly focused lasers to generate high quality electron beams in laser wakefield accelerators. In this scheme, the expansion of the laser beam after the focal position enlarges the size of wakefield bubble, which reduces the effective phase velocity of the wake and triggers injection of plasma electrons. This scheme injects a relatively long beam with high charge. The energy spread of the injected beam can be minimized if an optimal acceleration distance is chosen so that the beam chirp is suppressed. Particle-in-cell simulations indicate that electron beams with the charge on the order of nanocoulomb, the energy spread of ∼1%, and the normalized emittance of ∼0.1 mm mrad can be generated in uniform plasma using ∼100 TW laser pulses. An empirical formula is also given for predicting the beam charge. This injection scheme, with a very simple setup, paves the way toward practical high-quality laser wakefield accelerators for table-top electron and radiation sources.

DOI: 10.1103/PhysRevAccelBeams.26.091303

I. INTRODUCTION

Laser wakefield accelerators (LWFAs), proposed in 1979, have attracted wide attention due to their 3 to 4 orders of magnitude higher acceleration gradient than that of the conventional radio-frequency (rf) accelerators [1]. Recently, 8 GeV electron beams have been obtained by an LWFA within 20 cm acceleration distance [2]. Successive 24 h stable operation of LWFA and free-electron-laser based on LWFA have shown the bright prospect of this acceleration mechanism [3,4]. Although the output beam quality of the LWFA has been largely improved [5], there is still a certain distance for competing with the rf accelerators and satisfying the requirements of real applications. Obtaining high-quality stable electron bunches has always been a consistent goal of this research field.

In an LWFA, the ponderomotive force of a high intensity laser pulse off-axially expels the background electrons of an underdense plasma. Afterward they are pulled back by the nearly immobile ions and form an oscillating plasma wake wave following the drive laser. Under highly nonlinear conditions, the plasma electrons can be completely evacuated to form an ion column where strong acceleration field is formed. Bunched electrons can gain energies of several GeV within a few centimeters if they are placed at appropriate accelerating and focusing phases by a certain injection scheme. The injection scheme directly influences the quality of the electron bunch. In the past decades, many injection schemes have been proposed. The self-injection scheme uses the wave-breaking effect when the drive pulse reaches a certain threshold [6–11]. The optical injection schemes preaccelerate the electrons by the beat wave of counterpropagating laser pulses or the ponderomotive force of assistant laser pulses so that the injection threshold of the wakefield potential is reduced [12–15]. The ionization injection scheme uses the electric field of the driver to ionize inner-shell electrons of dopant gas atoms inside the wake to partially avoid the deceleration phase in the first half period of the wakefield so that these electrons are more likely to gain enough forward velocity for injection [16–19]. The density gradient injection scheme reduces the phase velocity of the wakefield by introducing a density decreasing region [5,20]. And the coaxial laser interference injection scheme reduces the phase velocity of the wakefield by the evolution of interference rings created by the tightly focused trigger laser which is coaxially propagating with the drive laser [21].

In this paper, we propose a new injection scheme that utilizes the evolution of a tightly focused drive laser to trigger the injection of background plasma electrons in LWFAs. Unlike typical self-injection due to the bubble evolution [9,22], our injection process is confined within a few Rayleigh range of the tightly focused drive laser, where the main reason of bubble evolution is the laser defocusing

*zengming@ihep.ac.cn
†lidz@ihep.ac.cn

after the focal point. Such laser defocusing leads to smooth expansion of the wakefield bubble and to the injection of electron beams with the charge on the order of nanocoulomb (nC), normalized emittance on the order of 0.1 mm mrad. At an optimal acceleration distance, the energy spread of the whole beam is minimized to the order of 1% due to the self-dechirping effect. Our scheme simultaneously produces high charge and small energy spread electron beams with a very basic setup of LWFA, thus has potential of wide applications.

II. A PHENOMENOLOGICAL THEORY

Previous studies have shown that electron beams with charges on the order of nC can be generated in underdense plasmas with densities of $n_p \sim 10^{19}$ to 10^{20} cm^{-3} by ~100 TW laser pulses with $w_0 \sim \lambda$, where w_0 is the laser waist, defined as the radius from the beam axis where the laser intensity drops to $\exp(-2)$ of the maximum value at the focal position, and λ is the laser wavelength, but the quality of the beams is relatively unsatisfactory [23,24]. The electron thermalization in underdense plasma is responsible for the broad energy spectrum, and the small w_0 is also disadvantageous to the energy chirp reduction of electron beam [24].

Here we explore the injection with $n_p \sim 10^{18}$ cm^{-3} and $4\ \mu\text{m} \lesssim w_0 \lesssim 10\ \mu\text{m}$ for $\lambda = 800$ nm. We consider the region with $da/dz < 0$, where $a = eA/m_e c^2$ is the normalized amplitude of the vector potential of the laser pulse (or the laser strength parameter), e is elementary charge, A is the amplitude of laser vector potential, m_e is the rest mass of electrons, c is the speed of light, and z is the longitudinal coordinate. For a tightly focused laser pulse with power ~100 TW, the ponderomotive force is strong enough to evacuate the background plasma electrons and create an electron-free bubble so that the laser defocuses within a short range as if it is in vacuum [25].

The transverse component of the ponderomotive force of a Gaussian laser pulse can be written as [26]

$$F_{pr} = -\frac{m_e c^2 a^2}{4\langle\gamma\rangle}\frac{\partial}{\partial r}\exp\left(-2\frac{r^2}{w^2}\right) = \frac{m_e c^2 a_0^2 w_0^2 r}{w^4\langle\gamma\rangle}\exp\left(-2\frac{r^2}{w^2}\right), \quad (1)$$

where a_0 is the value of a at focus in vacuum, $r = \sqrt{x^2+y^2}$ is the transverse position, $\langle\gamma\rangle$ is the Lorentz factor averaged in one laser cycle, w is the laser beam radius which is a function of z. Due to the effect of passive plasma lens for laser, the laser is focused more tightly in plasma than in vacuum [25,27], thus the actual evolution of the radius in the first laser envelope oscillation period can be approximately written as

$$w(z) = w_0\Gamma\sqrt{1+(z-z_{fe})^2/z_{\text{Re}}^2}, \quad (2)$$

where z_{fe} is the effective focal position in plasma, $z_{\text{Re}} = \pi w_0^2\Gamma^2/\lambda$ is the effective Rayleigh length. Neglect the energy loss of the laser, Γ can be written as

$$\Gamma = \frac{a_0}{a_{0e}} = \frac{w_{0e}}{w_0}, \quad (3)$$

where a_{0e} is the effective peak strength parameter and w_{0e} is the effective beam waist. We know that $\Gamma < 1$ if the focal position is inside the plasma, and $\Gamma = 1$ if it is outside. The focusing force in the bubble is [28]

$$F = -\kappa^2 r, \quad (4)$$

where $\kappa^2 = \omega_p^2 m_e/\alpha$ and ω_p is the plasma frequency. Generally $\alpha \geq 2$, and $\alpha = 2$ corresponds to the case of electron-free ion cavity. By balancing the ponderomotive force Eq. (1) and the focusing force Eq. (4), we can approximately get the bubble radius

$$r_b = \sqrt{\frac{w^2}{2}\ln\left(\frac{\Omega w_0^2 a_0^2}{w^4 k_p^2}\right)}, \quad (5)$$

where $\Omega = \alpha/\langle\gamma\rangle|_{r=r_b}$ and $k_p = \omega_p/c$ is the wave number of the plasma wave. For simplicity, we assume Ω is a constant. By taking derivative of Eq. (5), we know $dr_b/dz > 0$ if $\ln(\Omega w_0^2 a_0^2) - 2 > 4\ln w$. In other words,

$$w|_{z=z_{ie}} = \exp\left(-\frac{1}{2}\right)\left(\frac{\Omega w_0^2 a_0^2}{k_p^2}\right)^{\frac{1}{4}}, \quad (6)$$

where z_{ie} is the ending point of the bubble expansion. The transverse expansion of the bubble leads to longitudinal expansion also, which decreases the phase velocity of the wakefield and triggers the injection of the electrons into the bubble. By solving Eqs. (2) and (6), an optimistic estimation of the injection length is obtained

$$L_{\text{inj}} = z_{ie} - z_{fe} = z_{\text{Re}}\sqrt{\exp(-1)\frac{\sqrt{\Omega}a_0}{\Gamma^2 k_p w_0} - 1}. \quad (7)$$

III. PIC SIMULATIONS

A series of quasicylindrical particle-in-cell (PIC) simulations using the code WarpX with the pseudospectral analytical time domain solver have been carried out, where two azimuthal modes are used [29,30]. An example is illustrated in Figs. 1 and 2. The simulation box has the size of (50 μm, 50 μm) and the cell number of (3200, 512) in z

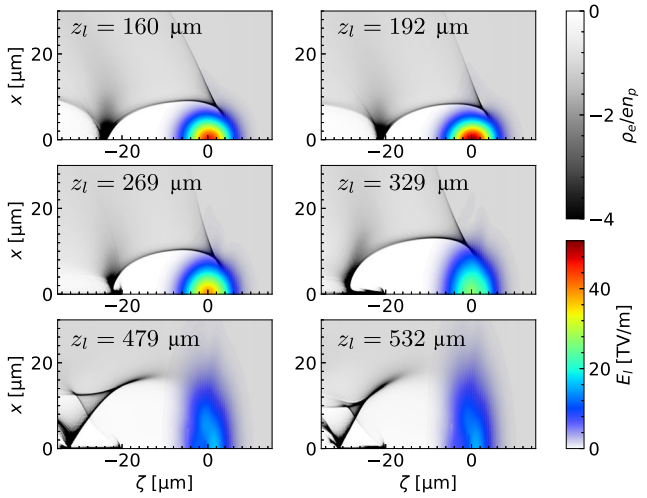

FIG. 1. The snapshots of the injection process in the plasma wakefield driven by a tightly focused laser. ρ_e is the electron density, n_p is the undisturbed plasma density, E_l is the profile of the electric field of the laser, and $\zeta = z - ct$ is the comoving coordinate. The laser center positions z_l are written for each of the subplots.

and r directions, respectively. The number of particles per cell along (z, r, θ) directions are $(2, 2, 4)$. The plasma density profile has a linear upramp from $z = 0$ to $z = 100$ μm, followed by a flattop with the density $n_p = 2 \times 10^{18}$ cm^{-3}. The laser pulse has $a_0 = 12$, $w_0 = 5$ μm, $\lambda = 800$ nm, $z_f = 200$ μm, and the pulse duration in full width half maximum $\tau = 20$ fs (the peak power is about 120 TW, and the energy is about 2.4 J). After the effective laser focal point ($z_{fe} \approx z_f$ for this case), a decreases, w increases, and r_b increases according to Eq. (5) which is in agreement with the simulation result as shown in Fig. 2(c). Later r_b decreases after the expansion ending point z_{ie} which can be obtained by solving Eq. (6). From Figs. 2(c) and 2(d) one can see that the longitudinal size of the bubble L_b is strongly correlated with its transverse size r_b. The increasing starting/ending points of L_b are almost the same as the increasing starting/ending points of r_b. Thus, the injection length, which is no longer than one increasing period of L_b, can be estimated by Eq. (7). At the tail of the beam, where the energy is initially lower, the higher acceleration gradient compensates the energy chirp of the whole beam. A high quality electron beam with the charge of $Q \approx 560$ pC, the root-mean-squared (rms) energy spread of 0.95% (obtained by Gaussian fit) and the normalized emittance of $\varepsilon_x = 0.34$ and $\varepsilon_y = 0.05$ mm mrad is generated at $z_l = 480$ μm as shown in Fig. 2(a), where z_l is the instant position of the laser pulse. A full 3D PIC simulation with the same laser and plasma parameters has been performed to reconfirm the electron beam quality parameters, which shows a similar result (see Sec. 1 of the Supplementary Material [31]). And for saving computational cost, all the following simulations are performed in the quasicylindrical mode.

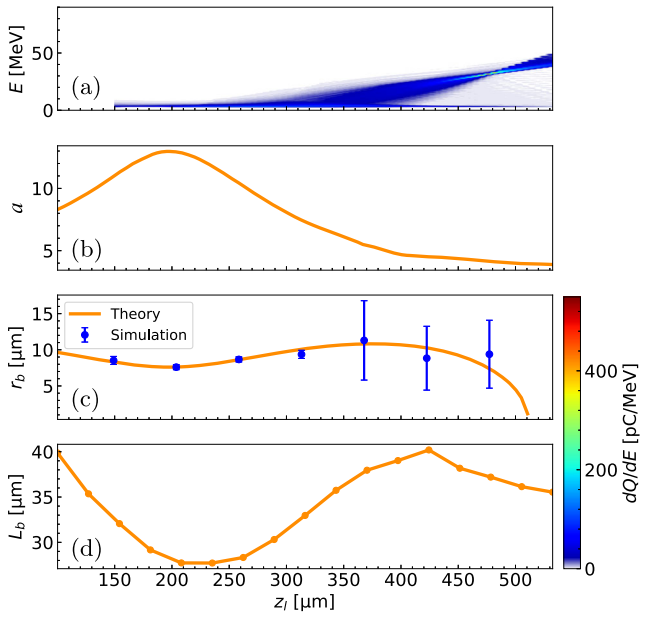

FIG. 2. The evolution of (a) the energy spectrum of the trapped electrons, (b) the laser strength parameter a, (c) the bubble radius r_b, and (d) the bubble length L_b vs the position of the laser center z_l. The error bar in (c) shows the range of the bubble sheath.

The beam charge is positively correlated with the laser intensity and plasma density. At different optimal acceleration lengths, which are on the order of hundred micrometers, the minimal energy spreads of the bunches are achieved, which are close to the slice energy spreads. In addition to the high-quality injection within the first bubble expansion period $z_{fe} < z < z_{ie}$, there can be low-quality injections at later bubble evolution periods due to laser-plasma interaction. These later injected beams can be separated from the high-quality injection due to their energy differences.

The case with $w_0 = 5$ μm has a relatively low beam energy because of the short accelerating length. With a relatively larger w_0, the beam energy and the optimal length increase as shown in Fig. 3. The optimal length is different for different cases, which means the plasma length adjustment is important to obtain a monoenergetic electron beam. The electron beam can have a monoenergetic peak in the spectrum with the central energy on the order of 100 MeV and the charge on the order of nanocoulomb. For example, the case with the laser energy of 7.84 J ($a_0 = 12$, $w_0 = 9$ μm) and the plasma density of 2×10^{18} cm^{-3} generates an electron beam with the energy of 250 MeV, the charge of 1.06 nC and the energy spread of 1.0% as shown in Fig. 3(c). The wave breaking leads to the density spike at the head of the electron beam, which has an attosecond duration and ultrahigh current ($\gtrsim$100 kA). The electrons injected after z_{ie} form the long tail of the beam, which broaden the energy spectra. More information for

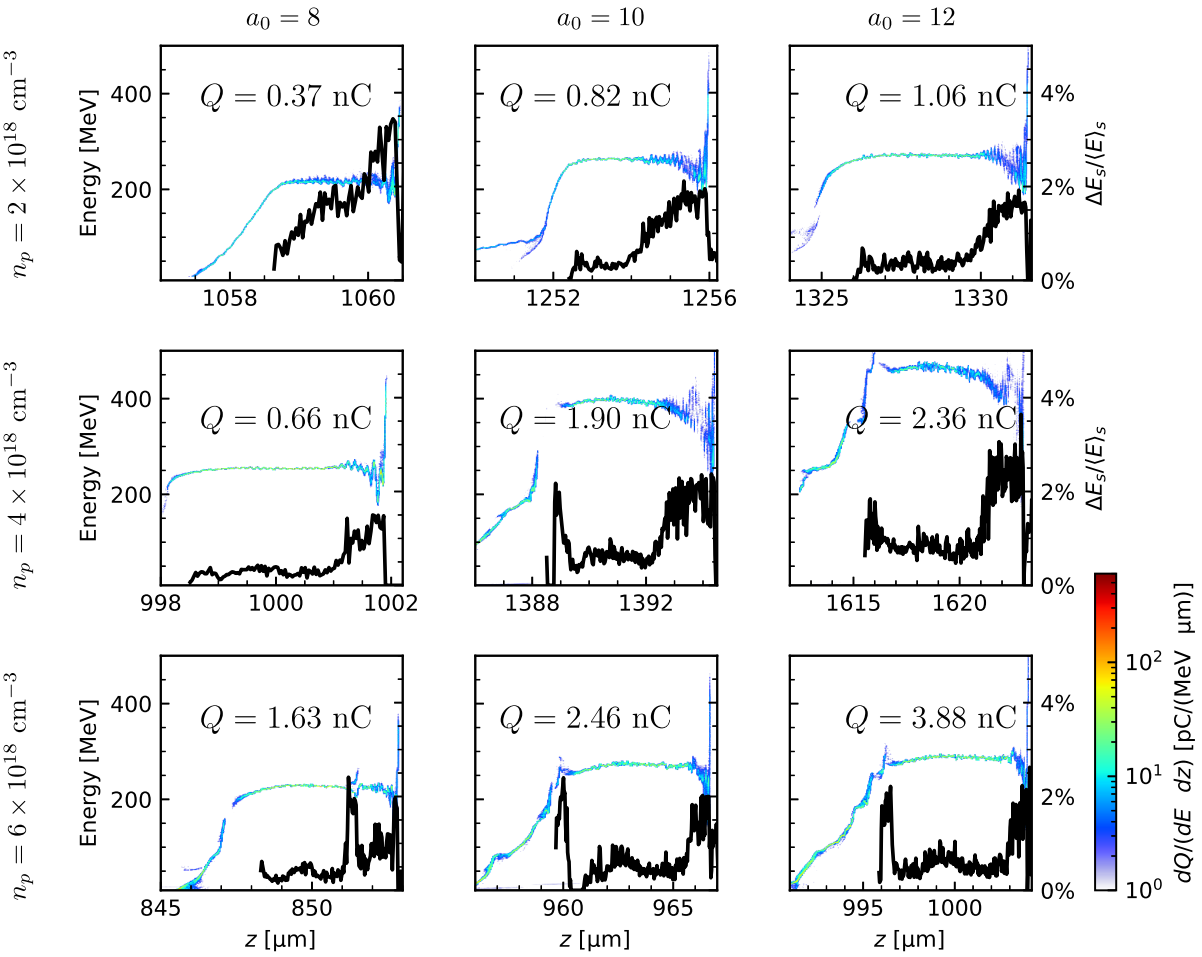

FIG. 3. The electron beam phase spaces at optimal acceleration lengths, which minimize the energy spreads, for fixed $w_0 = 9$ μm but different a_0 (shown at the top) and n_p (shown at the side). The laser pulse duration $\tau = 20$ fs for all cases. The laser pulse energies for $a_0 = 8$, 10 and 12 are 3.48, 5.44, and 7.84 J, respectively. The focal position is $z_f = 200$ μm. The slice energy spread $\Delta E_s/\langle E\rangle_s$ of electrons within the main peak of the energy spectrum is also plotted for each case, where ΔE_s is the rms energy spread of one slice, $\langle E\rangle_s$ is the average energy of one slice, and the slice width is the longitudinal cell size $\Delta z = 0.016$ μm.

$w_0 = 5$ μm and 7 μm cases are shown in Sec. 2 of the Supplementary Material [31].

The spectra and phase spaces of electron beams for different cases with a fixed laser power of 120 TW are shown in Fig. 4. The case with $w_0 = 2$ μm is more similar to the "cube of the pulse wavelength" injection mechanism [24]. For the moderately tightly focused cases, with 4 μm $\leq w_0 \leq$ 8 μm, the injection scheme is the scheme proposed in the present work. The injection positions are only between z_{fe} and z_{ie}, and each of these cases has one monoenergetic peak in the spectrum. The $w_0 = 10$ μm is the transition from our injection scheme to regular self-injection. For $w_0 > 10$ μm, the injections come from both $z < z_{fe}$ and $z_{fe} < z < z_{ie}$ positions, and the portion of injection from $z < z_{fe}$ becomes more significant when w_0 increases. The beam emittance and energy spread vs w_0 are plotted in Fig. 4(h), which show that the high quality beam, with both small emittance and small energy spread, can be generated with 4 μm $\leq w_0 \leq$ 10 μm.

IV. CHARGE SCALING

The amount of trapped charge is a key parameter for plasma based accelerators. For a static bubble under matched conditions, the number of electrons trapped in the accelerating phase can be estimated by equating the electromagnetic field energy in the ion cavity to the energy absorbed by the particles [32]. The injection scheme in this work is different, because the bubble is expanding. We look for an empirical formula for the injected beam in this section.

According to the simulation observations and previous experimental facts [33,34], we can reasonably assume that the amount of injected charge is linearly correlated with the production of the injection length L_{inj}, the plasma density n_p and the laser strength parameter at focus a_0, written as

$$Q = C \times L_{\text{inj}} n_p a_0, \tag{8}$$

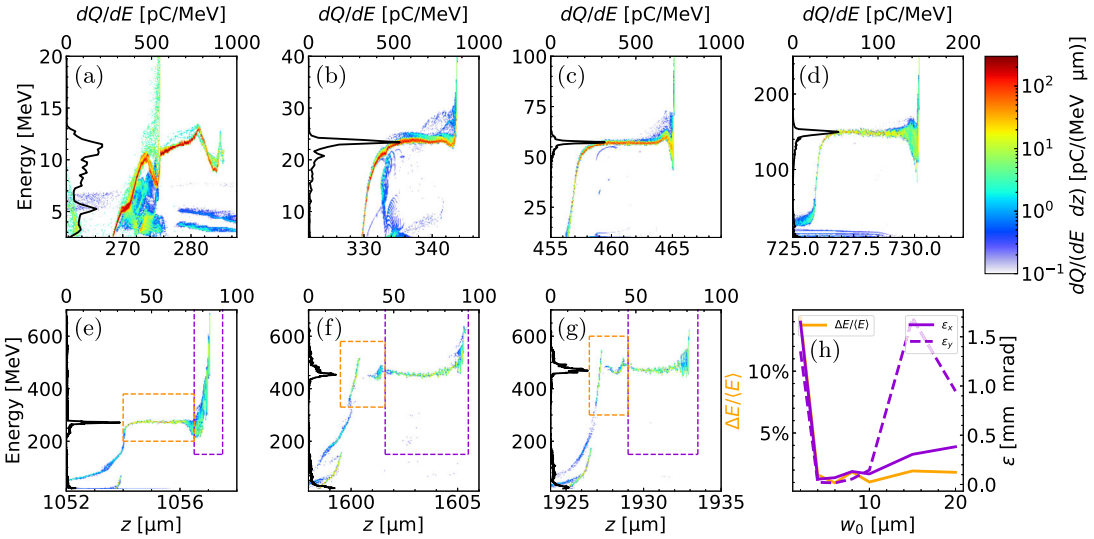

FIG. 4. The phase spaces and energy spectra of the injected electron beams for a fixed laser peak power of 120 TW, a fixed pulse duration of $\tau = 20$ fs (corresponding to a pulse energy of 2.4 J) and a fixed plasma density of $n_p = 4 \times 10^{18}$ cm^{-3}, while a_0 and w_0 from (a) to (g) are (30, 2 μm), (15, 4 μm), (10, 6 μm), (7.5, 8 μm), (6, 10 μm), (4, 15 μm), and (3, 20 μm), respectively. The focal position is $z_f = 200$ μm. The corresponding z_{fe} and z_{ie} for (a) to (g) are $(193, 259)$ μm, $(188, 303)$ μm, $(206, 356)$ μm, $(275, 437)$ μm, $(387, 546)$ μm, $(690, 833)$ μm, and $(937, 1043)$ μm, respectively. For 4 μm $\leq w_0 \leq 8$ μm cases, all of the electrons have the injection positions between z_{fe} and z_{ie}. For larger w_0, however, other injection positions can be majorities. In (e), (f), and (g), the electrons in the violet dashed rectangular boxes have the injection positions before z_{fe}, and the ones in the orange dashed rectangular boxes have the injection positions between z_{fe} and z_{ie}. In (h), the rms energy spreads of the beams obtained by fitting the main peaks of the energy spectra, and the emittance of the electrons within the main peaks are shown.

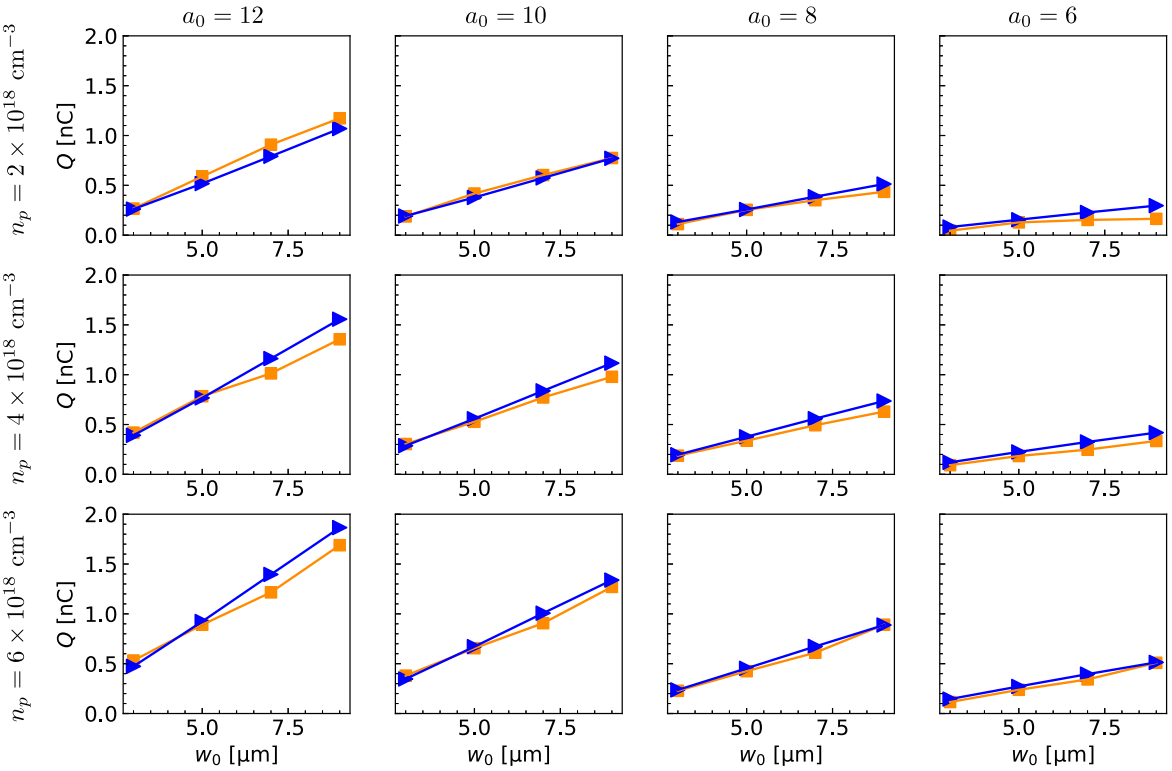

FIG. 5. The comparison between theory (blue curve) and simulation (yellow curve) of the injected beam charge vs w_0. The plasma densities are shown at the side and laser peak strength parameters a_0 are shown at the top. The laser pulse duration $\tau = 20$ fs for all cases. The focal position is $z_f = 200$ μm.

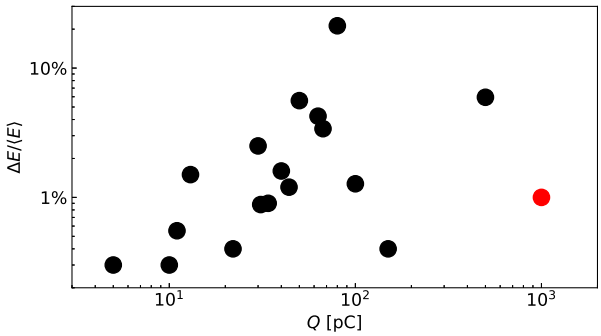

FIG. 6. The energy spread vs charge in previously published papers (black dots) and in this paper (red dot).

where C is an empirical constants. We notice that Γ and Ω also have to be determined to calculate Q. To simplify the model, we assume $\Omega = 2$ and do not consider the dependencies of Γ on the laser focal position z_f and the laser wavelength λ (fixed at 800 nm). Then Γ is a functions of n_p, a_0, and w_0 which can be approximately written in the following empirical form within a certain parameter space (see Sec. 3 of the Supplementary Material [31])

$$\Gamma \approx -\frac{n_p[10^{18}\ \mathrm{cm}^{-3}]}{20.16} + \frac{a_0}{100} - \frac{w_0[\mu\mathrm{m}]}{46.42} + 1.029. \quad (9)$$

The charges of the beams injected solely within $z_{fe} < z < z_{ie}$ for difference cases are shown in Fig. 5. One can see that the charge estimation Eq. (8) with $C = 1.19 \times 10^{-18}$ nC cm^2 has a good agreement with the simulations. Other simulations for checking the charge dependence on n_p and a_0 are shown in Sec. 4 of the Supplementary Material [31].

V. CONCLUSION

In conclusion, we have proposed an improved self-injection scheme in laser wakefield accelerators, which uses a tightly focused drive laser pulse to produce an electron beam with the charge on the order of nanocoulomb, the energy spread on the order of 1% and the normalized emittance on the order of 0.1 mm mrad with ~100 TW laser power. The key reason for such optimization is that the injection is induced by the laser defocusing shortly after the focal position, instead of by highly nonlinear laser evolution. Note the emittance is measured in plasma, which may increase in the transition from plasma to vacuum in general cases. We have also found an empirical formula for prediction the charge of the injected beam, which has good agreements with PIC simulations. This work is a follow-up of our previous studies on the simultaneous optimization of both the energy spread and the charge of LWFA produced electron beams [18,21]. As shown in Fig. 6, this proposed scheme has a significant multiparameter optimization for the beam energy spread and charge compared with previous results [5–7,15,35–43]. Such optimization, which can be realized by relatively simple experimental setup, may broaden the application range of LWFAs.

ACKNOWLEDGMENTS

This work is supported by Research Foundation of Institute of High Energy Physics, Chinese Academy of Sciences (Grants No. E05153U1, No. E15453U2, No. E329A1M1, No. Y9545160U2, and No. Y9291305U2), and Key Research Program of Frontier Sciences of Chinese Academy of Sciences (Grant No. QYZDJ-SSW-SLH004).

[1] T. Tajima and J. M. Dawson, Laser Electron Accelerator, Phys. Rev. Lett. **43**, 267 (1979).

[2] A. J. Gonsalves, K. Nakamura, J. Daniels, C. Benedetti, C. Pieronek, T. C. H. de Raadt, S. Steinke, J. H. Bin, S. S. Bulanov, J. van Tilborg, C. G. R. Geddes, C. B. Schroeder, C. Tóth, E. Esarey, K. Swanson, L. Fan-Chiang, G. Bagdasarov, N. Bobrova, V. Gasilov, G. Korn, P. Sasorov, and W. P. Leemans, Petawatt Laser Guiding and Electron Beam Acceleration to 8 gev in a Laser-Heated Capillary Discharge Waveguide, Phys. Rev. Lett. **122**, 084801 (2019).

[3] A. R. Maier, N. M. Delbos, T. Eichner, L. Hübner, S. Jalas, L. Jeppe, S. W. Jolly, M. Kirchen, V. Leroux, P. Messner, M. Schnepp, M. Trunk, P. A. Walker, C. Werle, and P. Winkler, Decoding Sources of Energy Variability in a Laser-Plasma Accelerator, Phys. Rev. X **10**, 031039 (2020).

[4] W. Wang, K. Feng, L. Ke, C. Yu, Y. Xu, R. Qi, Y. Chen, Z. Qin, Z. Zhang, M. Fang, J. Liu, K. Jiang, H. Wang, C. Wang, X. Yang, F. Wu, Y. Leng, J. Liu, R. Li, and Z. Xu, Free-electron lasing at 27 nanometres based on a laser wakefield accelerator, Nature (London) **595**, 516 (2021).

[5] L. T. Ke, K. Feng, W. T. Wang, Z. Y. Qin, C. H. Yu, Y. Wu, Y. Chen, R. Qi, Z. J. Zhang, Y. Xu, X. J. Yang, Y. X. Leng, J. S. Liu, R. X. Li, and Z. Z. Xu, Near-gev Electron Beams at a Few Per-Mille Level from a Laser Wakefield Accelerator via Density-Tailored Plasma, Phys. Rev. Lett. **126**, 214801 (2021).

[6] W. P. Leemans, B. Nagler, A. J. Gonsalves, C. Toth, K. Nakamura, C. G. R. Geddes, E. Esarey, C. B. Schroeder, and S. M. Hooker, GeV electron beams from a centimetre-scale accelerator, Nat. Phys. **2**, 696 (2006).

[7] X. Wang, R. Zgadzaj, N. Fazel, Z. Li, S. A. Yi, X. Zhang, W. Henderson, Y. Y. Chang, R. Korzekwa, H. E. Tsai, C. H. Pai, H. Quevedo, G. Dyer, E. Gaul, M. Martinez, A. C. Bernstein, T. Borger, M. Spinks, M. Donovan, V. Khudik, G. Shvets, T. Ditmire, and M. C. Downer, Quasi-monoenergetic laser-plasma acceleration of electrons to 2 GeV, Nat. Commun. **4**, 1988 (2013).

[8] W. P. Leemans, A. J. Gonsalves, H.-S. Mao, K. Nakamura, C. Benedetti, C. B. Schroeder, C. Tóth, J. Daniels, D. E. Mittelberger, S. S. Bulanov, J.-L. Vay, C. G. R. Geddes, and E. Esarey, Multi-gev Electron Beams from Capillary-Discharge-Guided Subpetawatt Laser Pulses in the Self-Trapping Regime, Phys. Rev. Lett. **113**, 245002 (2014).

[9] S. Kalmykov, S. A. Yi, V. Khudik, and G. Shvets, Electron Self-Injection and Trapping into an Evolving Plasma Bubble, Phys. Rev. Lett. **103**, 135004 (2009).

[10] S. Y. Kalmykov, S. A. Yi, A. Beck, A. F. Lifschitz, X. Davoine, E. Lefebvre, V. Khudik, G. Shvets, and M. C. Downer, Dark-current-free petawatt laser-driven wakefield accelerator based on electron self-injection into an expanding plasma bubble, Plasma Phys. Controlled Fusion **53**, 014006 (2010).

[11] S. Y. Kalmykov, A. Beck, S. A. Yi, V. N. Khudik, M. C. Downer, E. Lefebvre, B. A. Shadwick, and D. P. Umstadter, Electron self-injection into an evolving plasma bubble: Quasi-monoenergetic laser-plasma acceleration in the blowout regime, Phys. Plasmas **18**, 056704 (2011).

[12] C. B. Schroeder, P. B. Lee, J. S. Wurtele, E. Esarey, and W. P. Leemans, Generation of ultrashort electron bunches by colliding laser pulses, Phys. Rev. E **59**, 6037 (1999).

[13] G. Golovin, W. Yan, J. Luo, C. Fruhling, D. Haden, B. Zhao, C. Liu, M. Chen, S. Chen, P. Zhang, S. Banerjee, and D. Umstadter, Electron Trapping from Interactions between Laser-Driven Relativistic Plasma Waves, Phys. Rev. Lett. **121**, 104801 (2018).

[14] D. Umstadter, J. K. Kim, and E. Dodd, Laser Injection of Ultrashort Electron Pulses into Wakefield Plasma Waves, Phys. Rev. Lett. **76**, 2073 (1996).

[15] M. Zeng, A. Martinez de la Ossa, and J. Osterhoff, Ponderomotively assisted ionization injection in plasma wakefield accelerators, New J. Phys. **22**, 123003 (2020).

[16] M. Chen, Z.-M. Sheng, Y.-Y. Ma, and J. Zhang, Electron injection and trapping in a laser wakefield by field ionization to high-charge states of gases, J. Appl. Phys. **99**, 056109 (2006).

[17] A. Pak, K. A. Marsh, S. F. Martins, W. Lu, W. B. Mori, and C. Joshi, Injection and Trapping of Tunnel-Ionized Electrons into Laser-Produced Wakes, Phys. Rev. Lett. **104**, 025003 (2010).

[18] J. Wang, M. Zeng, X. Wang, D. Li, and J. Gao, Scissor-cross ionization injection in laser wakefield accelerators, Plasma Phys. Controlled Fusion **64**, 045012 (2022).

[19] M. Zeng, M. Chen, Z.-M. Sheng, W. B. Mori, and J. Zhang, Self-truncated ionization injection and consequent monoenergetic electron bunches in laser wakefield acceleration, Phys. Plasmas **21**, 030701 (2014).

[20] F. Massimo, A. Lifschitz, C. Thaury, and V. Malka, Numerical studies of density transition injection in laser wakefield acceleration, Plasma Phys. Controlled Fusion **59**, 085004 (2017).

[21] J. Wang, M. Zeng, D. Li, X. Wang, W. Lu, and J. Gao, Injection induced by coaxial laser interference in laser wakefield accelerators, Matter Radiat. Extremes **7**, 054001 (2022).

[22] X. Xu, T. N. Dalichaouch, J. Liu, Q. Ma, J. Pierce, K. Miller, X. Yan, and W. B. Mori, On the generation of ultrabright and low energy spread electron beams in laser wakefield acceleration in a uniform plasma, arXiv:2305.01866.

[23] H. Xu, W. Yu, P. Lu, V. K. Senecha, F. He, B. Shen, L. Qian, R. Li, and Z. Xu, Electron self-injection and acceleration driven by a tightly focused intense laser beam in an underdense plasma, Phys. Plasmas **12**, 013105 (2005).

[24] A. Zhidkov, T. Fujii, and K. Nemoto, Electron self-injection during interaction of tightly focused few-cycle laser pulses with underdense plasma, Phys. Rev. E **78**, 036406 (2008).

[25] M. Zeng, A. Martinez de la Ossa, K. Poder, and J. Osterhoff, Plasma eyepieces for petawatt class lasers, Phys. Plasmas **27**, 023109 (2020).

[26] P. Mora and T. M. Antonsen, Jr., Kinetic modeling of intense, short laser pulses propagating in tenuous plasmas, Phys. Plasmas **4**, 217 (1997).

[27] J. P. Palastro, D. Gordon, B. Hafizi, L. A. Johnson, J. Peñano, R. F. Hubbard, M. Helle, and D. Kaganovich, Plasma lenses for ultrashort multi-petawatt laser pulses, Phys. Plasmas **22**, 123101 (2015).

[28] W. Lu, C. Huang, M. Zhou, W. B. Mori, and T. Katsouleas, Nonlinear Theory for Relativistic Plasma Wakefields in the Blowout Regime, Phys. Rev. Lett. **96**, 165002 (2006).

[29] J.-L. Vay, A. Huebl, A. Almgren, L. D. Amorim, J. Bell, L. Fedeli, L. Ge, K. Gott, D. P. Grote, M. Hogan, R. Jambunathan, R. Lehe, A. Myers, C. Ng, M. Rowan, O. Shapoval, M. Thévenet, H. Vincenti, E. Yang, N. Zaïm, W. Zhang, Y. Zhao, and E. Zoni, Modeling of a chain of three plasma accelerator stages with the warpx electromagnetic pic code on gpus, Phys. Plasmas **28**, 023105 (2021).

[30] R. Lehe, M. Kirchen, I. A. Andriyash, B. B. Godfrey, and J.-L. Vay, A spectral, quasi-cylindrical and dispersion-free particle-in-cell algorithm, Comput. Phys. Commun. **203**, 66 (2016).

[31] See Supplemental Material at http://link.aps.org/supplemental/10.1103/PhysRevAccelBeams.26.091303 for more simulation results, including the 3D simulation, the cases with laser pulses with $w_0 = 5$ μm and 7 μm, obtaining the empirical formula for Γ and the charge dependence on n_p and a_0.

[32] W. Lu, M. Tzoufras, C. Joshi, F. S. Tsung, W. B. Mori, J. Vieira, R. A. Fonseca, and L. O. Silva, Generating multi-gev electron bunches using single stage laser wakefield acceleration in a 3d nonlinear regime, Phys. Rev. ST Accel. Beams **10**, 061301 (2007).

[33] S. Kuschel, M. B. Schwab, M. Yeung, D. Hollatz, A. Seidel, W. Ziegler, A. Sävert, M. C. Kaluza, and M. Zepf, Controlling the Self-Injection Threshold in Laser Wakefield Accelerators, Phys. Rev. Lett. **121**, 154801 (2018).

[34] D. H. Froula, C. E. Clayton, T. Döppner, K. A. Marsh, C. P. J. Barty, L. Divol, R. A. Fonseca, S. H. Glenzer, C. Joshi, W. Lu, S. F. Martins, P. Michel, W. B. Mori, J. P. Palastro, B. B. Pollock, A. Pak, J. E. Ralph, J. S. Ross, C. W. Siders, L. O. Silva, and T. Wang, Measurements of the Critical Power for Self-Injection of Electrons in a Laser Wakefield Accelerator, Phys. Rev. Lett. **103**, 215006 (2009).

[35] H. T. Kim, K. H. Pae, H. J. Cha, I. J. Kim, T. J. Yu, J. H. Sung, S. K. Lee, T. M. Jeong, and J. Lee, Enhancement of Electron Energy to the Multi-gev Regime by a Dual-Stage Laser-Wakefield Accelerator Pumped by Petawatt Laser Pulses, Phys. Rev. Lett. **111**, 165002 (2013).

[36] S. Jalas, M. Kirchen, P. Messner, P. Winkler, L. Hübner, J. Dirkwinkel, M. Schnepp, R. Lehe, and A. R. Maier, Bayesian Optimization of a Laser-Plasma Accelerator, Phys. Rev. Lett. **126**, 104801 (2021).

[37] G. Li, Q. Ain, S. Li, M. Saeed, D. Papp, C. Kamperidis, and N. A. M. Hafz, Control of electron beam energy-spread by beam loading effects in a laser-plasma accelerator, Plasma Phys. Controlled Fusion **62**, 055004 (2020).

[38] C. Rechatin, J. Faure, A. Ben-Ismail, J. Lim, R. Fitour, A. Specka, H. Videau, A. Tafzi, F. Burgy, and V. Malka, Controlling the Phase-Space Volume of Injected Electrons in a Laser-Plasma Accelerator, Phys. Rev. Lett. **102**, 164801 (2009).

[39] J. P. Couperus, R. Pausch, A. Köhler, O. Zarini, J. M. Krämer, M. Garten, A. Huebl, R. Gebhardt, U. Helbig, S. Bock, K. Zeil, A. Debus, M. Bussmann, U. Schramm, and A. Irman, Demonstration of a beam loaded nanocoulomb-class laser wakefield accelerator, Nat. Commun. **8**, 487 (2017).

[40] W. T. Wang, W. T. Li, J. S. Liu, Z. J. Zhang, R. Qi, C. H. Yu, J. Q. Liu, M. Fang, Z. Y. Qin, C. Wang, Y. Xu, F. X. Wu, Y. X. Leng, R. X. Li, and Z. Z. Xu, High-Brightness High-Energy Electron Beams from a Laser Wakefield Accelerator via Energy Chirp Control, Phys. Rev. Lett. **117**, 124801 (2016).

[41] M. Kirchen, S. Jalas, P. Messner, P. Winkler, T. Eichner, L. Hübner, T. Hülsenbusch, L. Jeppe, T. Parikh, M. Schnepp, and A. R. Maier, Optimal Beam Loading in a Laser-Plasma Accelerator, Phys. Rev. Lett. **126**, 174801 (2021).

[42] L. Ke, C. Yu, K. Feng, Z. Qin, K. Jiang, H. Wang, S. Luan, X. Yang, Y. Xu, Y. Leng, W. Wang, J. Liu, and R. Li, Optimization of electron beams based on plasma-density modulation in a laser-driven wakefield accelerator, Appl. Sci. **11**, 2560 (2021).

[43] M. Zeng, M. Chen, L. L. Yu, W. B. Mori, Z. M. Sheng, B. Hidding, D. A. Jaroszynski, and J. Zhang, Multichromatic Narrow-Energy-Spread Electron Bunches from Laser-Wakefield Acceleration with Dual-Color Lasers, Phys. Rev. Lett. **114**, 084801 (2015).